

Microscopic electroabsorption line shape analysis for Ga (AsSb)/GaAs heterostructures

C. Bückers, G. Blume, A. Thränhardt, C. Schlichenmaier, P. J. Klar, G. Weiser, S. W. Koch, J. Hader, J. V. Moloney, T. J. C. Hosea, S. J. Sweeney, J.-B. Wang, S. R. Johnson, and Y.-H. Zhang

Citation: *Journal of Applied Physics* **101**, 033118 (2007); doi: 10.1063/1.2433715

View online: <http://dx.doi.org/10.1063/1.2433715>

View Table of Contents: <http://scitation.aip.org/content/aip/journal/jap/101/3?ver=pdfcov>

Published by the [AIP Publishing](#)

Articles you may be interested in

[Interdiffusion of Indium in piezoelectric InGaAs/GaAs quantum wells grown by molecular beam epitaxy on \(111\) substrates](#)

J. Appl. Phys. **96**, 3702 (2004); 10.1063/1.1783611

[Ultrafast InGaAs/InGaAlAs multiple-quantum-well electro-absorption modulator for wavelength conversion at high bit rates](#)

Appl. Phys. Lett. **84**, 4268 (2004); 10.1063/1.1711165

[Molecular beam epitaxial growth of AlGaPSb and AlGaPSb/InP distributed Bragg reflectors on InP](#)

J. Vac. Sci. Technol. B **22**, 1468 (2004); 10.1116/1.1669600

[Linear electroabsorption in semi-insulating GaAs/AlGaAs asymmetric double quantum wells](#)

J. Appl. Phys. **86**, 3822 (1999); 10.1063/1.371293




[Enhanced electroabsorption in tensile-strained Ga_yIn_{1-y}As/Al_xIn_{1-x}As/InP quantum well structures, due to field-induced merging of light-hole and heavy-hole transitions](#)

Appl. Phys. Lett. **70**, 2855 (1997); 10.1063/1.119023



AIP | Journal of Applied Physics

Meet The New Deputy Editors

	Christian Brosseau		Laurie McNeil		Simon Phillpot
-------------------------------------------------------------------------------------	---------------------------	-------------------------------------------------------------------------------------	----------------------	---------------------------------------------------------------------------------------	-----------------------

Microscopic electroabsorption line shape analysis for Ga(AsSb)/GaAs heterostructures

C. Bückers

*Fachbereich Physik und Wissenschaftliches Zentrum für Materialwissenschaften,
Philipps-Universität Marburg, Renthof 5, D-35032 Marburg, Germany*

G. Blume

*Fachbereich Physik und Wissenschaftliches Zentrum für Materialwissenschaften,
Philipps-Universität Marburg, Renthof 5, D-35032 Marburg, Germany and Advanced Technology Institute,
University of Surrey, Guildford GU2 7XH, United Kingdom*

A. Thränhardt,^{a)} C. Schlichenmaier, P. J. Klar,^{b)} G. Weiser, and S. W. Koch

*Fachbereich Physik und Wissenschaftliches Zentrum für Materialwissenschaften,
Philipps-Universität Marburg, Renthof 5, D-35032 Marburg, Germany*

J. Hader and J. V. Moloney

*Arizona Center for Mathematical Sciences and Optical Sciences Center, The University of Arizona, Tucson,
Arizona 85721*

T. J. C. Hosea and S. J. Sweeney

Advanced Technology Institute, University of Surrey, Guildford GU2 7XH, United Kingdom

J.-B. Wang, S. R. Johnson, and Y.-H. Zhang

*Center for Solid State Electronics Research and Department of Electrical Engineering,
Arizona State University, Tempe, Arizona 85287-6206*

(Received 30 August 2006; accepted 27 November 2006; published online 12 February 2007)

A series of Ga(AsSb)/GaAs/(AlGa)As samples with varying GaAs spacer width are studied by electric-field modulated absorption (EA) and reflectance spectroscopy and modeled using a microscopic theory. The analysis of the Franz–Keldysh oscillations of GaAs capping layer and of the quantum-confined Stark shift of the lowest quantum well (QW) transitions shows the strong inhomogeneity of the built-in electric field indicating that the field modulation due to an external bias voltage differs significantly for the various regions of the structures. The calculations demonstrate that the line shape of the EA spectra of these samples is extremely sensitive to the value of the small conduction band offset between GaAs and Ga(AsSb) as well as to the magnitude of the internal electric field changes caused by the external voltage modulation in the QW region. The EA spectra of the entire series of samples are modeled by the microscopic theory. The good agreement between experiment and theory allows us to extract the strength of the modulation of the built-in electric field in the QW region and to show that the band alignment between GaAs and Ga(AsSb) is of type II with a conduction band offset of approximately 40 meV. © 2007 American Institute of Physics. [DOI: 10.1063/1.2433715]

I. INTRODUCTION

For a number of years, there has been considerable interest in finding suitable emitters at the so-called “telecommunication wavelengths,” defined by the dispersion and absorption minima of silica fibers at 1.3 and 1.55 μm , respectively. Vertical-cavity surface-emitting lasers¹ (VCSEL) have a circular beam profile and thus a superior beam quality, making them ideal for coupling into a fiber. Further benefits of VCSELs are low manufacturing costs and uncooled stable operation. High quality VCSELs can be realized using the GaAs/(AlGa)As material system where the excellent matching of the materials’ lattice constants, the high refractive index contrast, and the mature growth technology offer

high quality Bragg mirrors.² However, emitters at telecommunication wavelengths today are often InP-based (InGa)(AsP) structures, which cannot be grown on GaAs due to the high lattice mismatch. Possible GaAs-based alternatives include the dilute nitrides,³ InAs/GaAs quantum dots⁴ and, as is discussed here, Ga(AsSb) quantum wells where room temperature VCSEL operation was already demonstrated.⁵

An unresolved question remains the band alignment of GaAs_{1-x}Sb_x embedded between GaAs for $0.3 < x < 0.4$ which is the relevant Sb content for emission at telecommunication wavelengths. While holes are almost certainly confined in the Ga(AsSb) layer, electrons may or may not be, making the structure spatially direct (type I) or spatially indirect (type II), respectively. This has major implications for the lasing performance due to the changing electron-hole wave function overlap which determines the strength of the optical dipole matrix element.

^{a)}Electronic mail: angela.thraenhardt@physik.uni-marburg.de

^{b)}Present address: I. Physikalisches Institut, Justus-Liebig-Universität Gießen, Heinrich-Buff-Ring 16, D-35392 Gießen, Germany.

For a realistic prediction of optical spectra, we employ a fully microscopic theory⁶ based on the semiconductor Bloch equations.⁷ For semiconductor laser gain calculations, we have found a microscopic inclusion of carrier correlations indispensable.⁸ Calculations then reproduce experimental spectra without the need for phenomenological quantities like scattering times which depend on experimental parameters such as structure, temperature, and excitation density. The theory has been shown to yield good results in Ga(AsSb) (Ref. 9) as well as other telecommunication wavelength materials, i.e., the dilute nitrides.^{10,11}

In this article, we present a combined experiment—theory approach. We investigate a set of Ga(AsSb)/GaAs/(AlGa)As single quantum well (QW) samples in order to characterize the conduction band alignment between Ga(AsSb) and GaAs with an accuracy which has not been achieved previously. This level of accuracy is reached by analyzing the line shape of the modulation spectra in the region of the confined interband transitions instead of solely analyzing transition energies. The former approach is realized by a direct comparison of measured spectra and those calculated employing a fully microscopic theory. Earlier studies of this material system yielded controversial results. The analysis of the photoluminescence (PL) peaks as a function of spacer thickness indicated a weak type-I band alignment,¹² whereas a second investigation studying the excitation intensity dependent shift of the PL peak positions at low temperature inferred the interface to be weakly type II.¹³ There are several other publications supporting either type I (Refs. 14 and 15) or type II (Refs. 16–18) alignment. Here, we will show that a comparison of electroabsorption (EA) experiments with a microscopic theory clearly shows a type-II offset of 40 ± 20 meV in the conduction band.

II. EXPERIMENTAL DETAILS

The Ga(AsSb)/GaAs/(AlGa)As single QW samples investigated here were grown by molecular beam epitaxy on *n*-doped GaAs wafers. The nominally undoped epitaxial layers consist of a 400 nm GaAs buffer, two 75 nm Al_{0.25}Ga_{0.75}As barrier layers which enclose the QW region and a 50 nm GaAs capping layer. The QW consists of 7 nm GaAs_{1-x}Sb_x with adjacent GaAs spacers. The spacer thickness was varied between 0 and 6 nm yielding a set of five samples.¹⁹ The average Sb content in the quantum well is $x=0.357$ but growth related slight differences result in Sb contents as follows: no spacer 0.360 ± 0.001 , 1 nm spacer 0.356 ± 0.002 , 2 nm spacer 0.355 ± 0.003 , 3 nm spacer 0.358 ± 0.001 , and 6 nm spacer 0.361 ± 0.003 .¹²

For the EA and electroreflectance (ER) measurements the samples were coated with a thin layer of 5 nm of Pt, serving as a top contact, while the *n*-doped GaAs substrate was grounded. Thus a direct current (dc) bias voltage could be used to alter the internal field and an additional square wave alternating current voltage of typically 1.0 V was applied for modulation. The probe light, provided by a 100 W tungsten-halide lamp, was dispersed using a 1 m monochromator (B&M) with a band pass better than 1 meV and was focused onto the sample, which was mounted on the cold

finger of a He flow cryostat. The reflected (transmitted) light $R(I)$ and its modulation $\Delta R(\Delta I)$ were detected with a nitrogen-cooled Ge detector (North-Coast) and measured using a multimeter (Keithley 195A) and a lock-in amplifier (Stanford 830DSP), respectively.

In case of negligible changes of the reflectivity and the refractive index, the relative change of the transmitted intensity $\Delta I/I$ yields directly the field-induced change $\Delta\alpha$ of the absorption constant

$$\Delta\alpha = -\frac{\Delta I}{I d}, \quad (1)$$

where d is the thickness of the layer that generates the signal. This requirement is fulfilled for EA spectra in the vicinity of the lowest interband transitions of the (AlGa)As/GaAs/Ga(AsSb)/GaAs/(AlGa)As structure, i.e., the QW states. However, EA spectra cannot be acquired in the barrier region because of the strongly absorbing GaAs substrate. Therefore, ER spectroscopic measurements have been employed to measure signals from the GaAs capping and (AlGa)As barrier region and thus to obtain additional information about the structure. Further details on the setups can be found in Ref. 21.

III. MICROSCOPIC THEORY

For a realistic calculation of EA spectra, we need to compute the two corresponding absorption spectra at the internal electric fields determined by the sum and the difference, respectively, of external bias voltage and modulation voltage amplitude. In order to mimic the EA experiment, the two calculated absorption spectra are subtracted from each other.²³ The absorption is calculated from the imaginary part of the polarization⁶ P ,

$$\alpha(\omega) = \frac{\omega}{n_B c} \text{Im} \left\{ \frac{P(\omega)}{VE(\omega)} \right\}, \quad (2)$$

where c is the vacuum speed of light, n_B is the background index of refraction, V is the quantization volume and $E(\omega)$ is the electric field of the incident light. The macroscopic polarization may be calculated from the microscopic interband polarizations $P_{\mathbf{k}\lambda\lambda'} = \langle h_{-\mathbf{k}, \lambda'} e_{\mathbf{k}, \lambda} \rangle$ where e and h are electron and hole annihilation operators, respectively, λ and λ' are the electron and hole subband levels and \mathbf{k} is the in-plane momentum. The microscopic polarizations are computed from the semiconductor Bloch equations, see Ref. 24 for the multiband case. Coulomb interaction is fully taken into account which is important especially in a type-II structure where unconfined carriers may still be bound by electron-hole attraction.

The band structure is determined from an 8×8 - $\mathbf{k} \cdot \mathbf{p}$ theory.^{25,26} Figure 1 shows the electron (top) and hole (bottom) bandstructure of the 6 nm spacer structure at a temperature of $T=30$ K. We plot the five electron and four hole bands which are taken into account. The reason for the small spacing between the electron subbands lies in the very small offset in the conduction band at the GaAs/GaAsSb interface and will be explained in detail in Sec. V.

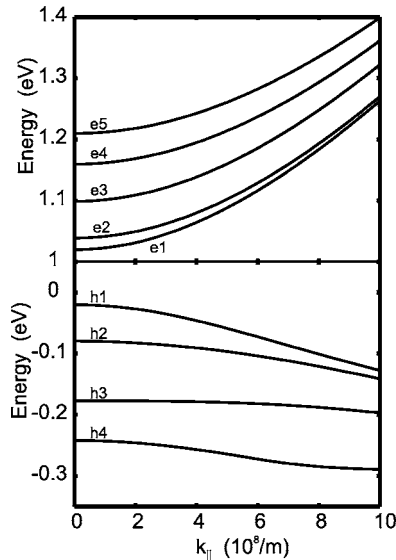


FIG. 1. Electron (top) and hole (bottom) bandstructure of the 6 nm spacer sample at $T=30$ K. Five electron and four hole bands are taken into account.

Electron-electron and electron-phonon scattering are treated in second Born and Markov approximation.²⁷ Sample parameters were taken from Refs. 28 and 29 with the exception of the bowing parameter where a value of 1.58 eV was used.¹²

IV. ANALYSIS OF THE BUILT-IN ELECTRIC FIELD

The employed square wave modulation voltage of 1.0 V corresponds nominally to an electric field of 15 kV/cm assuming that the entire voltage drop occurs in the intrinsic region (about 600 nm). However, this is usually not the case in multilayered structures where interface and surface charges are present, which lead to a partial screening of the external bias voltage. Here, we will present evidence that the built-in electric field at a constant external bias voltage varies for the different layers in the structures under study and will give some estimates of the internal field modulation caused by an external voltage modulation which will then be compared with values obtained from the theoretical analysis of the EA spectra discussed in Sec. V. Information about the internal electric fields can be obtained from an analysis of Franz–Keldysh oscillations (FKOs) as a function of bias voltage in bulk-like layers such as the GaAs capping layer of 50 nm (Ref. 20) and from an analysis of the “quantum confined Stark effect” (QCSE), i.e., the response of the lowest quantum well transition to the internal electric field changes caused by externally applied bias voltages.

The internal electric field F in a bulk-like layer can be deduced from corresponding FKOs using the following relation:

$$(E_n - E_g)^{3/2} = \frac{3}{8} \frac{Fqh}{\sqrt{2m^*}} n + \phi, \quad (3)$$

where E_g and m^* are the band gap and the reduced mass of GaAs, respectively ($m^*=0.05m_e$ where m_e is the free electron mass). E_n denotes the energy of the n th extremum of the

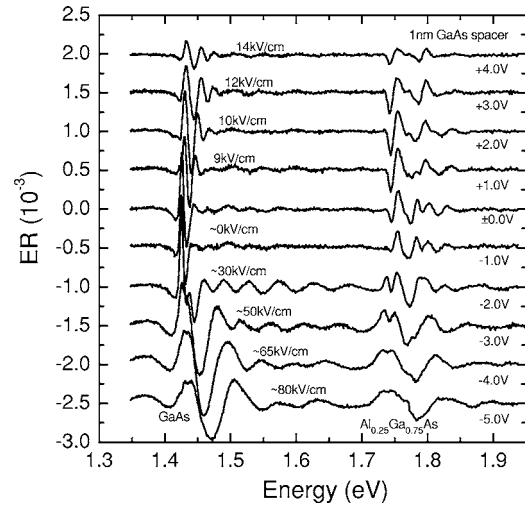


FIG. 2. Measured ER spectra of the GaAs capping and (AlGa)As barrier region of the sample with 1 nm GaAs spacers for different bias voltages as indicated on the right of each spectrum (vertically offset for clarity). One observes clear Franz–Keldysh oscillations above the band gap of GaAs at 1.42 eV.

FKOs, h is Planck’s constant, q is the charge of the electron, and ϕ is an arbitrary phase offset.

Figure 2 depicts ER spectra of the sample with 1 nm spacer obtained at room temperature in the vicinity of the GaAs and $\text{Al}_{0.25}\text{Ga}_{0.75}\text{As}$ band gaps for different external bias voltages. The FKOs in the GaAs ranging from 1.42 eV up to the (AlGa)As band gap near 1.75 eV are well pronounced. The change of the oscillation period with changing external bias voltage is clearly discernible. In contrast, the FKOs in the $\text{Al}_{0.25}\text{Ga}_{0.75}\text{As}$ region above 1.75 eV are confused by underlying signals arising from the spin-orbit split-off band of GaAs (≈ 1.76 eV) and thus not suitable for an analysis according to Eq. (3). The flatband situation in the GaAs capping layer is characterized by the disappearance of the FKOs which takes place at a bias voltages of about -0.5 ± 0.5 V. The bias voltage where the flatband situation occurs varies slightly from sample to sample by ± 1 V.

The results of the analysis of the FKOs in the GaAs region using Eq. (3) are presented in Fig. 3. The main graph shows plots of $(E_n - E_g)^{3/2}$ versus the index n of the FKO extrema for three different bias voltages. The deviation from the ideal linear behavior starting at indices $n > 6$ is a typical indication of an inhomogeneous field distribution in the structure. Nevertheless, restricting the analysis to the low index region alone allows one to extract a lower boundary for the internal field in this layer which is often used as a reasonable estimate of the field in the vicinity of the QW region. The inset shows the dependence of the extracted estimate of the built-in electric field versus bias voltage. A linear dependence is obtained for positive (forward) as well as negative (reverse) bias. The differences in the slope arise due to the asymmetry of the sample (i.e., n -doped GaAs substrate/intrinsic structure/Schottky Pt contact region).

Figure 4 shows EA absorption spectra of the same sample in the vicinity of the lowest QW transition in the Ga(AsSb)/GaAs/(AlGa)As region for various external bias voltages. Assuming a situation at a constant bias voltage

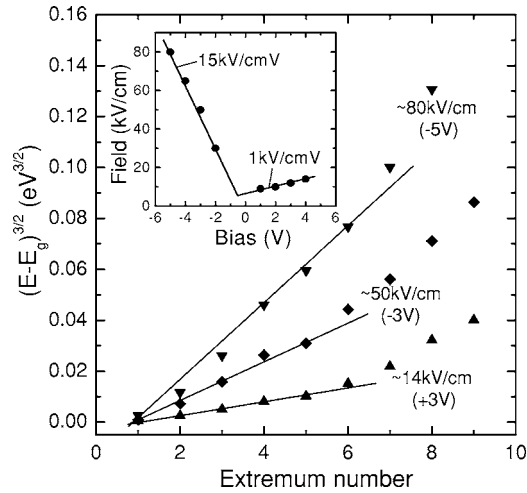


FIG. 3. Franz-Keldysh oscillation extrema plots of the GaAs region of the sample with 1 nm spacer for three selected biases, as indicated next to the data points. The electric field was inferred from the linear part of the slope. Inset: dependence of the built-in electric field in the GaAs capping region on applied bias voltage.

where the internal electric field in the QW region is zero, a change of the bias voltage will lead to a redshift of the lowest QW transition independent of the sign of the voltage change. This is a consequence of the QCSE.²² Therefore, the flatband situation in the QW region can be deduced from a plot of the lowest QW transition energy E_{QW} versus applied bias as shown in the inset of the figure. The application of a bias voltage of -5.8 V corresponding to the maximum of E_{QW} leads to the flatband situation in the QW region. It is worth noting that the flatband situation in the GaAs capping layer and in the QW region occur at very different applied biases which manifests the large field inhomogeneities in the samples. However, the bias voltage where the flatband situ-

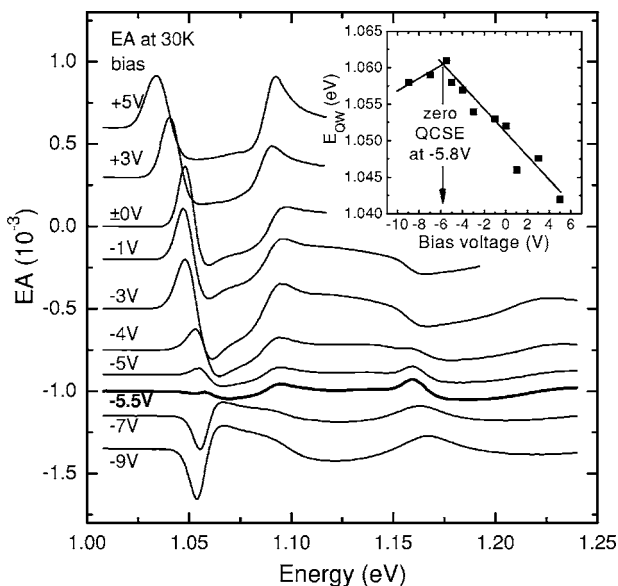


FIG. 4. Electroabsorption spectra in the vicinity of the lowest quantum well transition of the sample with 1 nm spacer for different bias voltages, as indicated next to the spectra. Inset: dependence of lowest QW transition energy E_{QW} on applied bias voltage. The flatband condition can be inferred from the apex of the data.

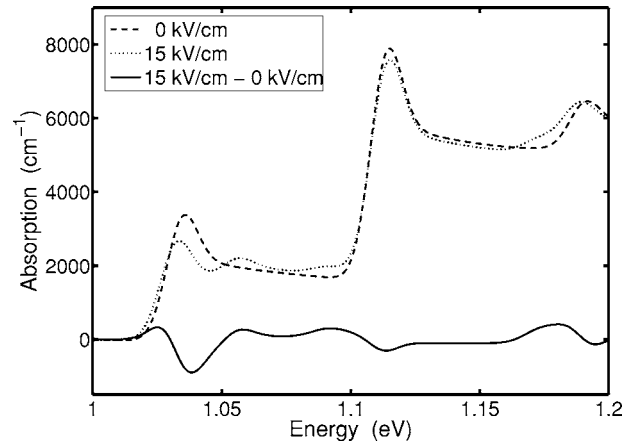


FIG. 5. Calculated linear absorption spectrum of the 6 nm spacer sample at $T=30$ K for fields of 0 kV/cm (dashed) and 15 kV/cm (dotted) and the electroabsorption spectrum obtained by calculating the difference between the two (solid).

ation in the QW region occurs varies throughout the series of samples, i.e., $+1$ V, ± 0 V, $+1$ V, and -1 V for spacers of 0, 2, 3, and 6 nm, respectively. The EA spectra for each sample in the vicinity of the flatband situation in the QW layers will be used in the analysis of the conduction band offsets in the following section.

V. DETERMINATION OF THE Ga(AsSb)/GaAs CONDUCTION BAND OFFSET

For the investigation of the optical properties of our Ga(AsSb) QW samples, we choose the method of electroabsorption which sensitively measures absorption changes induced by an electric field. In the experiments, the field switches between two different values and absorption changes are measured; imitating this in the calculation leads us to compute the absorption for two different electric fields and subtract the spectra from each other. Figure 5 shows the linear absorption calculated for the electric fields of 0 kV/cm (dashed) and 15 kV/cm (dotted) in the 6 nm spacer structure. The electric field applied in growth direction causes a redshift (linear field effect) as well as a loss of oscillator strength of the strong diagonal transitions $e1_h1$, $e2_h2$, while at the same time the formerly forbidden transitions like $e1_h2$ gain oscillator strength (quadratic field effect). Both effects are a manifestation of the QCSE introduced in Sec. IV. The solid line at the bottom of Fig. 5 shows the calculated EA signal where the two spectra were subtracted from each other. For the interpretation of the modulated spectra one generally has to bear in mind that a gain (loss) of oscillator strength leads to a peak (dip) while a shift results in a dispersive line shape. For instance, the redshift of the lowest transition causes a dispersive type signal which is rendered asymmetric by the loss of oscillator strength of the lowest transition. Formerly forbidden transitions like the $e2_h1$ or $e1_h2$ gain oscillator strength when an electric field is applied which is manifested in positive signals. The figure also shows that gain and loss of oscillator strength of the various interband transitions are correlated and that this correlation is clearly reflected in the EA spectra. In a conventional analysis of the modulated spectrum, where the line shape is fitted by

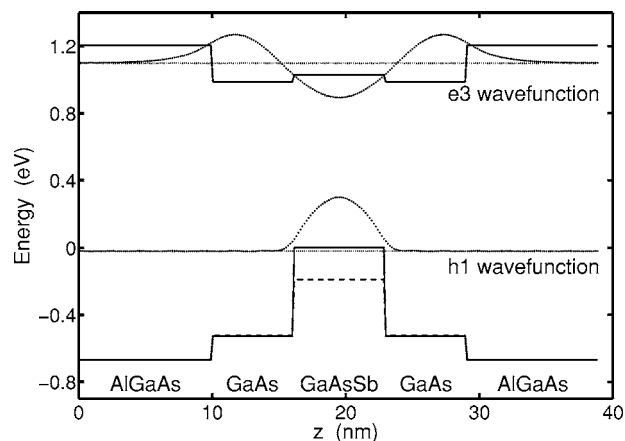


FIG. 6. Electron and hole confinement potentials for the sample with 6 nm GaAs spacers at $T=30$ K. A type-II offset of 40 meV is assumed. The dashed line shows the light hole confinement. Also shown are the first heavy hole and third electron wave functions. Since the effective quantum well width for the electron is about three times that for the holes, these wave functions have good overlap and a high oscillator strength, see Fig. 7.

employing a sum of independent oscillators representing the individual interband transitions, the correlation between the oscillator strengths of the various transitions is difficult to extract and hard to quantify whereas in the microscopic theory it occurs naturally.

The considerable amount of information about the band alignment hidden in the relative oscillator strength of the various interband transitions in such a complicated multilayer structure of (AlGa)As/GaAs/Ga(AsSb)/GaAs/(AlGa)As is demonstrated exemplarily in Figs. 6 and 7. A special feature of the 6 nm spacer sample considered here is the large oscillator strength of the $e3_h1$ transition even without an applied electric field. It arises due to the almost flat conduction band offset between GaAs and Ga(AsSb) at this alloy composition, i.e., the electron barriers are not formed by the GaAs, but by the (AlGa)As. Holes, on the other hand, are already well confined within GaAs_{0.65}Sb_{0.35}, i.e., GaAs acts as a hole barrier. The confinement potential

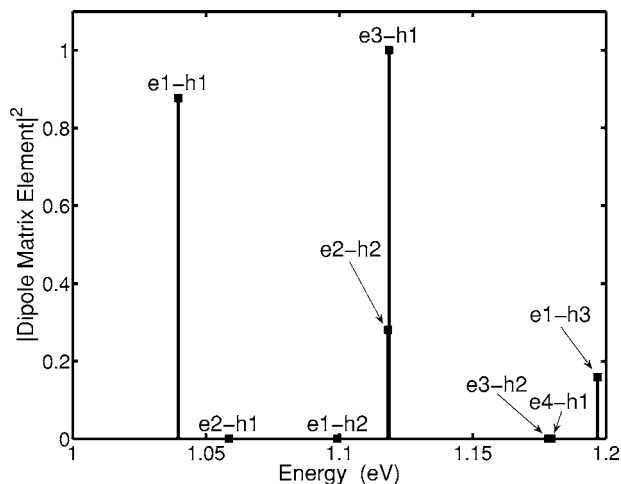


FIG. 7. Square of the dipole matrix element versus the transition energy for the sample with 6 nm GaAs spacers at $T=30$ K. Both dipole matrix element and transition energy are taken at zero in-plane electron momentum, i.e., at the band minimum. A type-II offset of 40 meV is assumed.

and $e3$ and $h1$ wave functions of the structure with 6 nm GaAs spacers at $T=30$ K are shown in Fig. 6 assuming a weak type-II offset of 40 meV. The effective well width for the electrons includes the spacers and is about three times larger than the effective well width for the holes (7 nm QW+2.6 nm spacer), leading to an almost perfect overlap of first hole and third electron wave functions resulting in a strong $e3_h1$ transition. Figure 7 shows the squared oscillator strength for all transitions for the field-free case (flatband in each layer of the QW region). The large effective well width for electrons also causes a high number of electron states to be important in the calculation, see Figs. 1 and 7. For instance, four electronic and three hole subband states are required to compute a correct absorption spectrum up to energies of about 1.2 eV without an electric field. Applying a field increases the number of states due to the QCSE-induced redshift. In the field-free case of Fig. 7, parity-forbidden transitions have an oscillator strength of strictly zero. The $e1_h1$ transition shows a high oscillator strength; however, $e2_h2$ and $e3_h1$ add up to make an even stronger absorption at higher energies.

We will now address the determination of the correct conduction band offset by comparing measured EA spectra and those calculated using our microscopic approach. However, some remarks need to be made beforehand. It should be noted that, for this particular band structure situation, where almost the entire gap difference between GaAs and Ga(AsSb) is to be found in the valence band and the conduction band alignment is close to a negligible offset situation, the distinction between a type-I and a type-II alignment (talking about offsets in the conduction band of only about $\pm 5\%$ of the gap difference!) is extremely challenging. Conventional approaches in modulation spectroscopy, where the modulated spectra are fitted with line shape models to extract the transition energies which are then compared to calculated values, will fail for several reasons: (i) The material parameters for the GaAs_{1-x}Sb_x, including the variation of the band gap with composition x or the strain parameters such as the elastic compliances and the deformation potentials, are not known to an extent of accuracy to enable a discussion of changes of the transition energies due to confinement of ± 40 meV on an absolute energy scale of about 1 eV set by the band gap. (ii) The transition energies will only weakly depend on the offset variation discussed earlier and, moreover, these differences are within the uncertainties of the calculation caused by the uncertainties in the material parameters. (iii) Because of the large effective well width in the conduction band and the enhancement in oscillator strength of the nondiagonal transitions due to the different effective well widths for electrons and holes, the transitions contributing significantly to the EA spectrum are very densely spaced in energy compared to their broadening. In a situation where broad oscillators overlap, conventional fitting methods for extracting energy position, linewidth, and oscillator strength usually fail. For these three reasons, another approach for determining the offset situation is required which preferably should not depend on absolute transition energies, but instead depends on the relative conduction band offset situation only. A quantity which fulfills this requirement is the

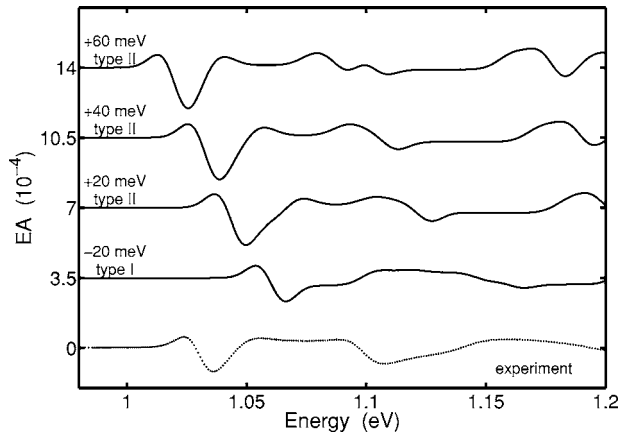


FIG. 8. Comparison of experimental (dotted) and theoretical (solid) electro-absorption spectra for the sample with 6 nm GaAs spacers. The calculations are for different band offsets. The spectra are vertically displaced for clarity. The temperature is $T=30$ K. Clearly, the line shape changes strongly with confinement in the calculations and shows a good agreement with experiment for the 40 meV type-II offset. The experiment is for an applied voltage bias of -1 V (flatband), the theory corresponds to an internal electric field variation of 4 kV/cm in the vicinity of the flatband situation.

overlap of the electron and hole wave functions confined in the structure and thus also the oscillator strength of the corresponding transitions and its electric field response which in turn determine the line shape of the EA spectrum. Again to emphasize this point, the differences between calculated and measured spectra on an absolute energy scale cannot serve as a criterion in the offset determination as these are within the standard deviation of the literature values for the band gap of Ga(AsSb).

Figure 8 shows a comparison of calculated EA spectra with a measurement taken in the vicinity of the flatband situation for the QW layers. Since the experiment gives the relative change of transmitted intensity $\Delta I/I$, the calculated $\Delta\alpha$ spectra were multiplied by the width of the active region; thus signal magnitudes in theory and experiment are comparable. The best quantitative agreement in terms of signal strength was achieved for an internal electric field modula-

tion of 4 kV/cm. This value is of the same order of magnitude as the values determined from the analysis of the FKOs in the GaAs capping layers (see Sec. IV). Different conduction band offsets of +60 meV (type II), +40 meV (type II), +20 meV (type II), and -20 meV (type I) were assumed in the calculation. An inhomogeneous broadening of 12 meV is included. Obviously, the assumption of a weak type-II offset of about +40 meV gives the best agreement: The line shape of the first and second resonance (around 1.04 and 1.12 eV, respectively) are both quite well reproduced and the energetic distance between these signals of about 0.073 eV matches the experiment, too, thus giving a clear indication of a type-II offset. The calculation assuming an offset of 20 meV shows a shoulder in the first resonance which is not visible in experiment. Using higher offsets of about 60 meV yields two dips in the second resonance which do not occur in experiment. We conclude that the offset is 40 ± 20 meV at a temperature of 30 K and in the following, assume an offset of +40 meV.

To verify the significance of the derived conduction band offset value and the predictive power of the microscopic theory, we also calculated EA spectra of the same sample for different bias voltages (Fig. 9) and of samples with different GaAs spacer thickness (Fig. 10). Figure 9 shows the experimental spectra for different external bias voltages (left picture). On the right, the corresponding calculated spectra are plotted. Again, theory reproduces the main features seen in the measurement, corroborating the offset of +40 meV. In addition, the dashed lines in Fig. 9 show calculations for a higher modulation field of 15 kV/cm, namely the field F derived by simply assuming $F=U/d$ where U is the applied bias voltage and d is the width of the undoped layers, i.e., a value considerably higher than that obtained from the analysis of the FKOs, see Sec. IV. Their signal magnitudes are about ten times stronger than the magnitudes of the measured spectra at 0 and -1 V, whereas the magnitudes yielded for the lower modulation field of 4 kV/cm are comparable to the experimental ones. Also, the relative height and width do not

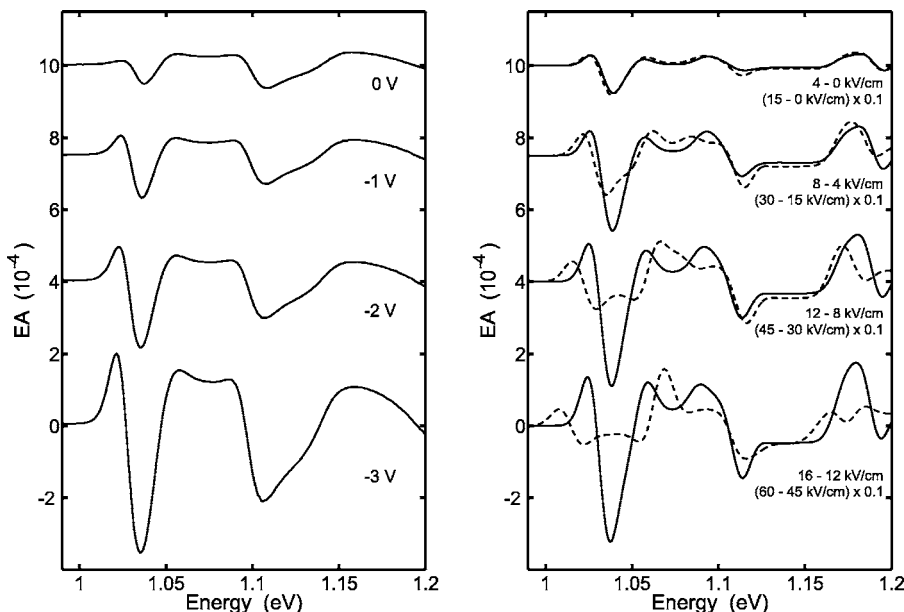


FIG. 9. Comparison of experimental (left) and theoretical (right) electro-absorption spectra for the sample with 6 nm GaAs spacers. An offset of 40 meV type II is assumed. Shown are the results for different dc fields, which are vertically displaced for clarity. The temperature is $T=30$ K. The dashed lines show calculations for the electric field we would expect without screening, scaled by a factor of 0.1. Clearly, theory-experiment agreement is better for a small field modulation.

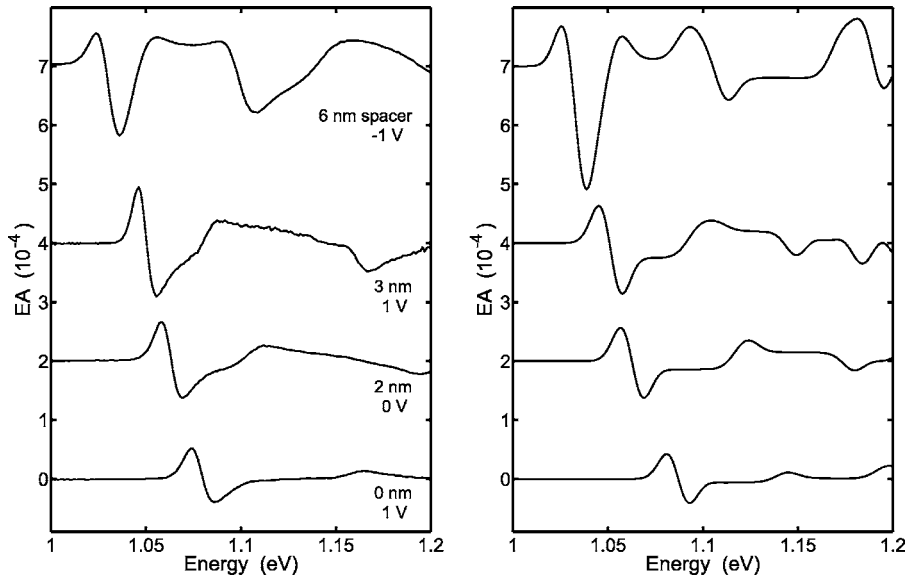


FIG. 10. Comparison of experimental (left) and theoretical (right) electroabsorption spectra for the sample set. The spectra are vertically displaced for clarity. An offset of 40 meV type II is assumed. The temperature is $T=30$ K.

match for the high modulation signal. Moreover, the line-shapes of the spectra calculated for different modulation voltages differ considerably: For instance, considering the first resonance for the bottom curve measured at -3 V, the signal calculated for the high modulation field clearly shows a shoulder while the experimental and the lower modulation signal display one clear dip. On the one hand, this demonstrates that the choice of the correct internal field modulation is extremely important for obtaining a good agreement with the experimental spectra. On the other hand, this means that the comparison between microscopic theory and experiment can be used to extract further information about the internal electric field in such complicated layered structures,²³ which is not accessible by an FKO analysis.

Figure 10 shows an overview of the measured and calculated EA spectra for the samples with 6, 3, and 2 nm and without GaAs spacers in the vicinity of the flatband situation for the QW layers. Again, for the reasons discussed earlier, the energy positions of the resonances are slightly different in theory and experiment, but more importantly a good agreement between the line shapes of experimental and theoretical spectra is obtained, verifying the conclusion that the samples are weakly type II. The deviations in linewidth between theory and experiment toward higher energies, in particular for the samples with the thicker spacer layers, is due to an increase of the inhomogeneous broadening with energy which is a commonly observed effect^{30,31} and is not accounted for in the calculation.

VI. CONCLUSIONS

We investigate a series of GaAs_{0.65}Sb_{0.35} QW samples embedded in Al_{0.25}Ga_{0.75}As with GaAs spacers of different width (0–6 nm) on both sides of the QW. The EA spectra were calculated employing a microscopic theory with no free parameters except for a phenomenological inhomogeneous broadening. The line shape of the EA spectra is very sensitive to the choice of the conduction band offset between GaAs and GaAs_{0.65}Sb_{0.35} as well as to the assumed modulation of the internal electric field. Comparison of the internal

electric field response to applied bias voltage determined by analysis of the FKOs in bulk-like layers and by the analysis of the QCSE in the QW region demonstrate that the built-in electric field is inhomogeneous throughout the structure. Accounting for the field inhomogeneities by analyzing the EA spectra in the vicinity of the flatband situation for the QW layers, we were able to conclude that the band alignment between GaAs and GaAs_{0.65}Sb_{0.35} is of type II with a conduction band offset of 40 ± 20 meV at a temperature of 30 K. Employing a full microscopic theory in the analysis of modulation spectra of complex multilayered structures offers new possibilities for extracting band structure and band alignment parameters with an accuracy far exceeding that of conventional analysis methods based on least-square line shape fitting with oscillator models.

ACKNOWLEDGMENTS

The authors acknowledge funding by the Deutsche Forschungsgemeinschaft (DFG) through the research group 483 “Metastable Compound Semiconductor Systems and Heterostructures,” by AFOSR (F49620–02–1–0380), the senior scientist award of the Humboldt foundation, and the EPSRC (UK) for providing funding under Grant No. GR/T21516/01.

- ¹K. Iga, IEEE J. Sel. Top. Quantum Electron. **6**, 1201 (2000).
- ²W. W. Chow, K. D. Choquette, M. H. Crawford, K. L. Lear, and G. R. Hadley, IEEE J. Quantum Electron. **33**, 1810 (1997).
- ³G. Steinle, H. Riechert, and A. Yu. Egorov, Electron. Lett. **37**, 93 (2001).
- ⁴Y. H. Chang *et al.*, IEEE Photonics Technol. Lett. **18**, 847 (2006).
- ⁵P. Dowd *et al.*, Electron. Lett. **39**, 987 (2003).
- ⁶H. Haug and S. W. Koch, *Quantum Theory of the Optical and Electronic Properties of Semiconductors*, 4th ed. (World Scientific, Singapore, 2004).
- ⁷M. Lindberg and S. W. Koch, Phys. Rev. B **38**, 3342 (1988).
- ⁸M. Hofmann *et al.*, Appl. Phys. Lett. **78**, 3009 (2001).
- ⁹C. Schlichenmaier, S. W. Koch, and W. W. Chow, Appl. Phys. Lett. **81**, 2944 (2002).
- ¹⁰C. Schlichenmaier *et al.*, Appl. Phys. Lett. **86**, 081903 (2005).
- ¹¹A. Thränhardt *et al.*, Appl. Phys. Lett. **86**, 201117 (2005).
- ¹²J.-B. Wang *et al.*, Phys. Rev. B **70**, 195339 (2004).
- ¹³G. Blume, T. J. C. Hosea, S. J. Sweeney, S. R. Johnson, J.-B. Wang, and Y.-H. Zhang, IEE Proc.: Optoelectron. **152**, 110 (2005).
- ¹⁴A. D. Prins, D. J. Dunstan, J. D. Lambkin, E. P. O’Reilly, A. R. Adams, R.

- Pritchard, W. S. Truscott, and K. E. Singer, *Phys. Rev. B* **47**, 2191 (1993).
- ¹⁵R. T. Senger *et al.*, *Appl. Phys. Lett.* **83**, 2614 (2003).
- ¹⁶M. Dinu, J. E. Cunningham, F. Quochi, and J. Shah, *J. Appl. Phys.* **94**, 1506 (2003).
- ¹⁷G. Liu, S. L. Chuang, and S. H. Park, *J. Appl. Phys.* **88**, 5554 (2000).
- ¹⁸G. Blume, T. J. C. Hosea, and S. J. Sweeney, *Phys. Status Solidi A* **202**, 1244 (2005).
- ¹⁹For further growth details see S. R. Johnson *et al.*, *J. Cryst. Growth* **251**, 521 (2003).
- ²⁰H. J. Kolbe, C. Agert, W. Stolz, and G. Weiser, *Phys. Rev. B* **59**, 14896 (1999).
- ²¹K. Satzke, H. G. Vestner, G. Weiser, L. Goldstein, and A. Perales, *J. Appl. Phys.* **69**, 7703 (1991).
- ²²D. A. B. Miller, D. S. Chemla, T. C. Damen, A. C. Gossard, W. Wiegmann, T. H. Wood, and C. A. Burrus, *Phys. Rev. Lett.* **53**, 2173 (1984).
- ²³A. Thränhardt, H. J. Kolbe, J. Hader, T. Meier, G. Weiser, and S. W. Koch, *Appl. Phys. Lett.* **73**, 2612 (1998).
- ²⁴A. Thränhardt, S. Becker, C. Schlichenmaier, I. Kuznetsova, S. W. Koch, J. Hader, J. V. Moloney, and W. W. Chow, *Proc. SPIE* **6115**, 61150W (2006).
- ²⁵W. W. Chow and S. W. Koch, *Semiconductor-Laser Fundamentals* (Springer, Berlin, 1999).
- ²⁶J. Hader, S. W. Koch, J. V. Moloney, and E. P. O'Reilly, *Appl. Phys. Lett.* **76**, 3685 (2000).
- ²⁷A. Girndt, F. Jahnke, A. Knorr, S. W. Koch, and W. W. Chow, *Phys. Status Solidi B* **202**, 725 (1997).
- ²⁸I. Vurgaftman, J. R. Meyer, and L. R. Ram-Mohan, *J. Appl. Phys.* **89**, 5815 (2001).
- ²⁹Landolt-Börnstein, in *Numerical Data and Functional Relationships in Science and Technology, Vol. 41: Semiconductors*, edited by O. Madelung, U. Rössler, M. Schulz (Springer, Berlin, 2002).
- ³⁰B. Kramer, K. Maschke, P. Thomas, and J. Treusch, *Phys. Rev. Lett.* **25**, 1020 (1970).
- ³¹B. Kramer, K. Maschke, and P. Thomas, *J. Phys. (France)* **33**, C3-157 (1972).